Synthesis of Ordered Ultra-long Manganite Nanowires via Electrospinning Method *

Jun Zheng(郑俊)[1], Kai Du(杜恺)[1], Di Xiao(肖迪)[1], Zheng-Yang Zhou(周正阳)[1], Wen-Gang Wei(魏文刚)[1,2], Jin-Jie Chen(陈金杰)[1], Li-Feng Yin(殷立峰)[1,3**], Jian Shen(沈健)[1,3**]

[1]*State Key Laboratory of Surface Physics and Department of Physics, Fudan University, Shanghai 200433*
[2]*College of Physics Science and Information Engineering, Hebei Normal University, Shijiazhuang 050024*
[3]*Collaborative Innovation Center of Advanced Microstructures, Nanjing 210093*

(Received 6 March 2016)

We develop a new electrospinning method to prepare ultra-long ordered $La_{1-x}Sr_xMnO_3$ (LSMO) nanowires. The length is up to several centimeters and is only limited by the size of the collector. The well-ordered straight-line structure ensures the transport measurement, which is impossible to be carried out for the random nanowires fabricated by the traditional electrospinning method. Magnetic and transport measurements indicate that the physical properties of the LSMO nanowires depend sensitively on the doping concentration. At the optimum doping, the LSMO wires are ferromagnetic at room temperature with a metal-insulator transition temperature close to room temperature. Magnetic force microscopy studies are also performed to provide a microscopic view of these ultra-long nanowires.

PACS: 75.47.Lx, 61.46.Km, 73.63.−b DOI: 10.1088/0256-307X/33/9/097501

Complex oxides under spatial confinement continue to be at the forefront of condensed matter physics. Emergent phenomena, such as discrete resistivity steps,[1,2] dynamics of metal-insulator transition,[3] double metal-insulator transition,[4] ferromagnetic-metallic edge state,[5] and quantum phase slip[6] have been found in colossal magnetoresistance manganite nanowires and high T_c super conductor cuprite nanowires, which are absent in bulk and thin films. Complex oxide nanowires are also the building blocks of new functional electronic devices[7] and nanosensors.[8] Therefore, researchers have developed numerous techniques to fabricate these kinds of complex oxide nanowires. In general, they can be divided into two categories, either top-town methods like photolithography,[1,6,9] or bottom-up methods like self-assembling growth.[10,11] Among these methods, electrospinning is very unique because it is the only method that can produce massive continuous wires with a diameter down to the nanometer size.[12] However, the disordered fiber structures hinder the application in device fabrications due to the fact that it is almost impossible to separate a single nanowire from the disordered fibers while keeping the length. The first attempt to produce ordered nanowires of simple oxides by electrospinning was very successful,[10] while it is still a challenge for complex oxides.[13] The advantages of the electrospinning method are that the stoichiometry of nanowires can be easily controlled by the precursor solutions, and the morphologies can be tuned by electrospinning and calcination processes. The high aspect ratio and the highly porous fibrous nanostructures of electrospun nanowires are suitable for those applications that need massive nanowires, such as ultraviolet photodetection,[14] photo catalysis[15] and energy storage,[16] while they are not suitable for single wire based applications.[17]

To overcome this limitation, in this Letter, a modified electrospinning method is developed to fabricate ultra-long and separated nanowires of complex oxides $La_{1-x}Sr_xMnO_3$ (LSMO) with a length up to centimeters. This new method is quite simple, and can be utilized for any materials. Magnetic and transport measurements indicate that the physical properties of the LSMO nanowires depend sensitively on the doping concentration. At the optimum doping, the Curie temperature (T_c) of LSMO nanowires is 365 K, while the metal-insulator transition temperature (T_p) is only 275 K. The discrepancy between magnetic and transport measurements has been regarded as the grain boundary effect.[18] Magnetic force microscopy (MFM) measurements have been performed to provide a microscopic proof.

The electrospinning method utilizes a strong electric field to stretch charged precursor solution into fibers.[12,19] As shown in Fig. 1(a), the typical setup of traditional electrospinning device consists of high voltage power supply, injection pump, syringe with a stainless steel needle, and metal collector. The needle of the syringe is connected to the high-voltage power supply, and the bottom collector is grounded. With a proper viscosity, the precursor droplets can be extruded out by the injection pump into the strong electric field. The charges on the surface of droplets will overcome the surface tension and shot jets of precursor into linear shape. When the charged jets accelerated by the electric field reach the grounded collector, the length has been stretched hundreds of times and thus the width will be significantly smaller than the

*Supported by the National Basic Research Program of China under Grant Nos 2016YFA0300700, 2013CB932901 and 2014CB921104, the National Natural Science Foundation of China under Grant Nos 11274071 and 11504053, and the Shanghai Municipal Natural Science Foundation under Grant No 11ZR140260.

**Corresponding author. Email: lifengyin@fudan.edu.cn; shenj5494@fudan.edu.cn

© 2016 Chinese Physical Society and IOP Publishing Ltd

original diameter of the needle. Due to the bending instability,[20] the jets of precursor will crash on the surface of collector and then result in a disordered fiber structure.

LSMO nanostructures by electrospinning are fabricated with a precursor solution containing polyvinylpyrrolidone (PVP). Here $La(NO_3)_3{\cdot}6H_2O$, $Sr(NO_3)_2$ and $Mn(NO_3)_3{\cdot}3.8H_2O$ nitrates with 0.67:0.33:1 molar ratio of La:Sr:Mn are used as the starting materials. After the nitrates are dissolved in deionized water, the viscosity of the solution is formulated by PVP powder, and subsequently the solution is stirred for 12 h before loaded into the syringe. The distance between the syringe and the grounded metal pad is 15 cm and the voltage is 15 kV. After the electrospinning progress, the collected LSMO wires are heated to 700℃ in a flowing oxygen environment for 3 h to evaporate PVP, followed by additional 10 h annealing at 900℃ to ensure crystallization.

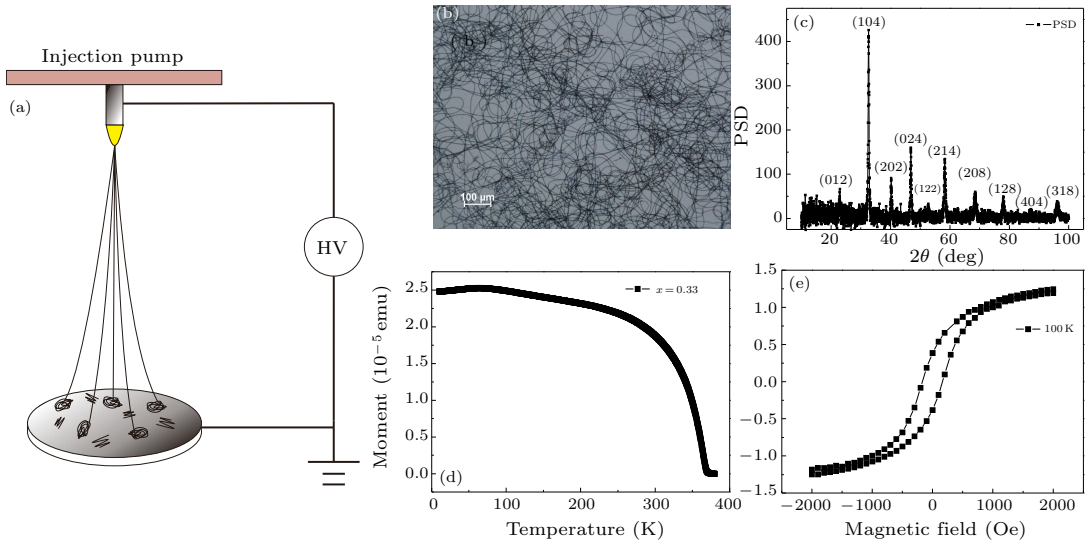

Fig. 1. (a) Schematic diagram of the traditional electrospinning setup. HV stands for the high-voltage power supply. (b) Optical microscopy view of LSMO nanofibers. (c) XRD patterns show that the LSMO ($x = 0.33$) nanofibers are polycrystalline with the rhombohedral ($R\bar{3}C$) structure. (d) The 100 Oe field cooling curve indicates that T_c is around 365 K. There appears a kink around 50 K. (e) Hysteresis loops measured at 100 K.

Figure 1(b) is the optical microscope picture of typical final products fabricated by the traditional electrospinning method. LSMO nanofibers with random orientation are entangled by each other, however the width is still uniform (around 1.75 μm±0.18 μm). The crystal structure is determined by lab based x-ray diffraction (XRD) with Cu $K\alpha$ radiation. The XRD patterns in Fig. 1(c) shows that the LSMO ($x = 0.33$) nanofibers are polycrystalline with a rhombohedral ($R\bar{3}C$) structure. The lattice parameters are determined to be $a = b = c = 0.38725$ nm, which is the same value as the bulk material.

The magnetic properties are measured by a superconducting quantum interference device magnetometer (SQUID of Quantum Design). The 100 Oe field cooling curve in Fig. 1(d) indicates that the Curie temperature is around 365 K, which is quite close to that of the bulk (370 K).[21] To our surprise, a small kink appears around 50 K, which indicates that a second magnetic phase transition takes place. The typical hysteresis loop is shown in Fig. 1(e). Due to the random orientation of LSMO nanofibers, there is no well-defined magnetic easy axis.

We have shown the best results based on the traditional electrospinning method. Now we will discuss how the ultra-long and separated nanowires could be achieved. Let us analyze the electrospinning process again to see why it results in a disordered fiber structure. As sketched in Fig. 1(a), before reaching the collector, all of the jets of the precursor are actually separated straight lines. The crash only takes place on the surface of the bottom collector. Therefore, we can collect the middle part of jets to achieve separated nanowires. Such an idea can be realized by adding a tilted silicon wafer as the second collector between the top syringe needle and the bottom collector (Fig. 2(a)). Due to the electrostatic repulsion, only slight jets will be attracted by the silicon wafer while the rest of the jets will still crash on the bottom collector, as described above. The electrostatic repulsion also makes sure that the nanowires on the silicon wafer are separated and remain well ordered. As shown in Fig. 2(b), all three of the nanowires are almost parallel to each other, and the typical spacing is around 0.7 mm.

The tilting angle of the silicon wafer plays the most important role in the final morphology. As sketched in Fig. 1(a), the trajectory of jets during electrospinning forms a cone-like structure. We usually put the silicon wafer in the middle of the syringe needle and the bottom collector, which has been proved to be the best position, and then tilt the silicon wafer until it is parallel to the side surface of the cone. If the tilting angle is not sufficient, then the crash of the jets is unavoidable because there is an effective projection area in the trajectory of the jets. However, if it tilts

too much, then no jets of precursor could be caught by the silicon wafer.

Figure 2(d) is an optical microscope picture of an ultra-long LSMO nanowire. The image can only show part of the nanowire, since the total length is up to 4.3 cm, which is already beyond the upper limit of optical microscope's field of view. The width of the nanowires can be tuned by changing the pinhole diameter or the nitrate weight percentage of the precursor. As shown in Figs. 2(e)–2(g), the width can range from 400 nm to 20 μm. The length is only limited by the size of silicon wafer (2 inch). The spacing of the nanowires can be adjusted by the precursor viscosity. The typical weight percentage of PVP in precursor is 30%. However, with a larger viscosity (35% weight percentage of PVP), fewer jets can be caught in one shot and the spacing can be even larger than 1 cm.

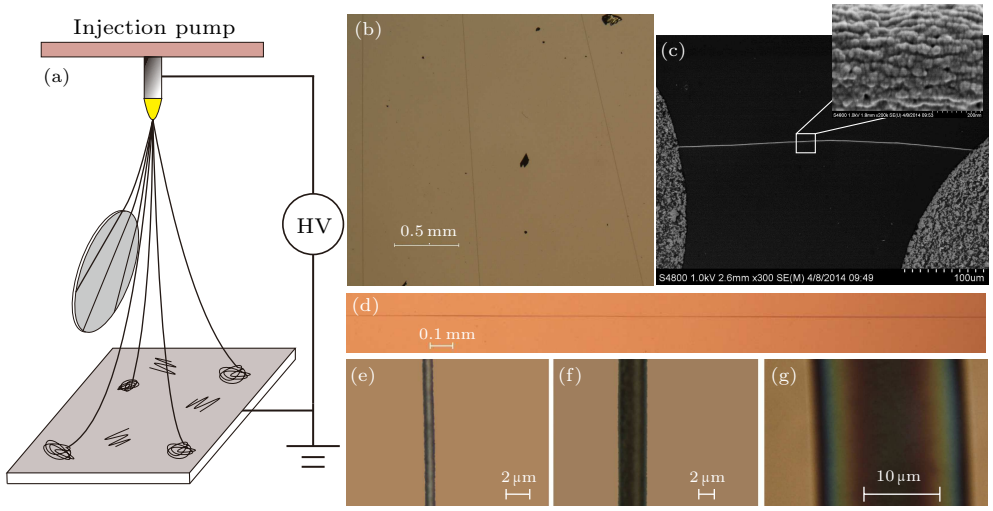

Fig. 2. (a) Schematic diagram of the modified electrospinning setup. A tilted silicon wafer is used as the second collector in the middle of the top syringe needle and the bottom collector. (b) Optical microscope image of ordered nanowires. The typical spacing is around 0.7 mm. (c) SEM image of a single LSMO nanowire for the transport measurements with silver epoxy electrodes on both the sides. The magnification image shows that the nanowire is constructed of textured nanocrystal, ranging from 15 nm to 30 nm. (d) Optical microscope image of 4.3-cm-long LSMO nanowire. The width of the nanowire can be tuned via growth parameters: (e) 400 nm, (f) 3.1 μm, and (g) 20 μm.

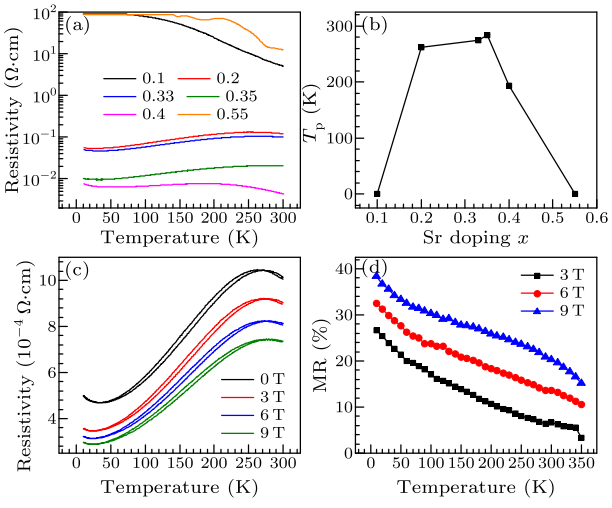

Fig. 3. (a) Zero-field ρ–T curves of LSMO nanowires, showing that the MIT is sensitively dependent on Sr doping. Here the efficient sizes (length, width) of each nanowire are $x = 0.1$ (0.85 mm, 1.3 μm), $x = 0.2$ (0.80 mm, 0.80um), $x = 0.33$ (0.97 mm, 0.89 μm), $x = 0.35$ (0.91 mm, 0.86um), $x = 0.4$ (2.5 mm, 1.56 μm), $x = 0.55$ (0.68 mm, 1.15 μm), respectively. (b) The optimum doping appears at $x = 0.35$. (c) The ρ–T curves of LSMO ($x = 0.33$) show a second MIT around 50 K; , the temperature where the M–T curve shows a kink (Fig. 1(d)). This implies that the grain boundaries are AFI phase. This AFI phase can be melted by the external magnetic field and results in the magnetoresistance curves increasing with cooling as shown in (d).

The ultra-long length and the huge spacing distance of ordered nanowires offer a great convenience for the electronic transport measurements. Figure 2(c) is the scanning electron microscope (SEM) image of a single LSMO nanowire for the transport measurements with silver epoxy electrodes on both sides. The magnification image in Fig. 2(c) illustrates that the nanowire is constructed of textured polycrystal, which is consistent with the XRD measurements. The size of the nanocrystal ranges from 15 nm to 30 nm.

The transport measurements are carried out in the physical property measurement system (PPMS of Quantum Design). As shown in Figs. 3(a) and 3(b), the metal-insulator transition of electrospinning LSMO nanowires sensitively depends on Sr doping. Either Sr rich ($x = 0.55$) or Sr deficient ($x = 0.1$) doping, LSMO nanowires are an insulator in the entire temperature range. Between them, metal-insulator transition (MIT) shows up and the optimum doping appears at 0.35, which gives the highest MIT temperature (275 K). However, it is still lower than the magnetic transition temperature (365 K), probably due to the grain boundary effect.[18] The LSMO nanowires do not have an epitaxial relationship with the silicon wafer substrate, and thus the effect of the substrate on the orbital ordering[22,23] may be negligible. The silicon wafer is coated with a layer of SiO_2, which should also suppress interfacial diffusion between the

substrate and the LSMO nanowires.[24] Considering the fact that the nanowires have a polycrystalline structure, we believe that the grain boundary effect may have a more profound influence on the physical properties of the nanowires. This is evidenced by the fact that another MIT emerges around 50 K (Fig. 3(c)); that is, the temperature where the M–T curve shows a kink in Fig. 1(d). This implies that the grain boundaries are an antiferromagnetic insulator (AFI) with the Neel temperature around 50 K, caused by the defects such as oxygen vacancy or lattice distortion. Figure 3(c) shows that the AFI phase of the grain boundaries can be melted by the external magnetic field, thus the magnetoresistance curves in Fig. 3(d) increase with cooling.

To further check this phase separation scenario, MFM measurements are carried out in PPMS with a scanning probe microscope (Attocube). Figure 4(a) is the morphology of LSMO nanowire measured by the atomic force microscope (AFM), showing 2 μm in width and 550 nm in height. The MFM image (Fig. 4(b)) at 300 K (the temperature lower than T_c) shows that the nanowire is really phase separated, whereas negative signals in red color stand for the attractive force, thus ferromagnetic metallic (FMM) state.[5] The paramagnetic insulator (PI) states are labelled in green. The typical FMM domain size is around 600 nm. This phase separation picture can explain why T_p is significantly lower than T_c, since the conducting path is blocked by the PI phase. When further cooling to 240 K (Fig. 4(c)), all of the FMM domains are merged. However, no obvious phase separation can be observed at 40 K (Fig. 4(d)), due to the fact that the nominal resolution of MFM is only 20 nm, and the strong stray field of FMM domains could also smear out the AFI signal of the domain boundary.

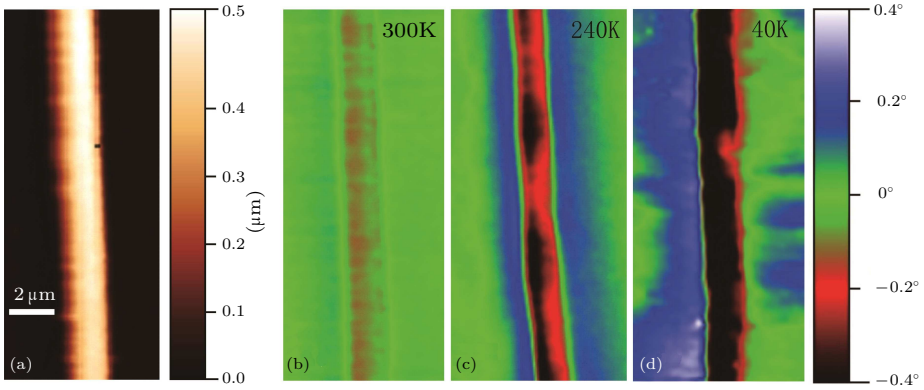

Fig. 4. (a) AFM measurement shows that the LSMO nanowire ($x = 0.33$) is 2 μm in width and 550 nm in height. (b) MFM measurement shows that the nanowire has a nanometer size phase separation at 300 K, whereas the red color stands for the FMM state. The PI states are labelled in green. This phase separation picture can explain why T_p is significant lower than T_c, since the conducting path is blocked by the PI phase. (c) With further cooling to 240 K, all the FMM domains are merged. (d) The magnetic signal becomes much stronger at 40 K.

In summary, we have developed a new electrospinning method to produce ultra-long and separated nanowires of complex oxides. This method is very simple and convenient, and it can be utilized in producing ultra-long nanowires for any materials. The only limitation is that the nanowires are polycrystalline, which is due to the lattice mismatch between silicon wafer and LSMO specimen during annealing. This can be solved by using a lattice matched perovskite wafer, such as $SrTiO_3$ or $LaAlO_3$, since our method does not require that the wafer is conducting.

References

[1] Zhai H Y et al 2006 *Phys. Rev. Lett.* **97** 167201
[2] Singh-Bhalla G et al 2009 *Phys. Rev. Lett.* **102** 077205
[3] Ward T Z et al 2009 *Phys. Rev. Lett.* **102** 087201
[4] Roosen D et al 2008 *Phys. Rev. Lett.* **100** 087201
[5] Du K et al 2015 *Nat. Commun.* **6** 6179
[6] Xu K and Heath J R 2008 *Nano Lett.* **8** 3845
[7] Xia Y et al 2003 *Adv. Mater.* **15** 353
[8] Wang Z L 2004 *Annu. Rev. Phys. Chem.* **55** 159
[9] Shen J et al 2013 *Chin. Phys.* B **22** 017501
[10] Li D et al 2003 *Nano Lett.* **3** 1167
[11] Li L et al 2013 *Solid State Commun.* **171** 46
[12] Wu H, Pan W, Lin D D and Li H P 2012 *J. Adv. Ceram.* **1** 2
[13] Jugdersuren B, Kang S, DiPietro R S, Heiman D, McKeown D, Pegg I L and Philip J 2011 *J. Appl. Phys.* **109** 016109
[14] Wu H, Sun Y, Lin D D, Zhang R, Zhang C and Pan W 2009 *Adv. Mater.* **21** 227
[15] Zhang R, Wu H, Lin D D and Pan W 2009 *J. Am. Ceram. Soc.* **92** 2463
[16] Mai L Q, Xu L, Han C H, Xu X, Luo Y Z, Zhao S Y and Zhao Y L 2010 *Nano Lett.* **10** 4750
[17] Guo H W, Noh Joo H, Dong S, Rack P D, Gai Z, Xu X S, Dagotto E, Shen J and Ward T Z 2013 *Nano Lett.* **13** 3749
[18] Jang J W, Lee C E, Lyu S C, Lee T J and Lee C J 2004 *Appl. Phys. Lett.* **84** 2877
[19] Tan J S, Long Y Z and Li M M 2008 *Chin. Phys. Lett.* **25** 3067
[20] Yarin A L, Koombhongse S and Reneker D H 2001 *J. Appl. Phys.* **89** 3018
[21] Urushibara A, Moritomo Y, Arima T, Asamitsu A, Kido G and Tokura Y 1995 *Phys. Rev.* B **51** 14103
[22] Cui B, Song C, Mao H J, Wu H Q, Li F, Peng J J, Wang G Y, Zeng F and Pan F 2015 *Adv. Mater.* **27** 6651
[23] Cui B, Song C, Gehring G A, Li F, Wang G Y, Chen C, Peng J J, Mao H J, Zeng F and Pan F 2015 *Adv. Funct. Mater.* **25** 864
[24] Kourkoutis L F, Song J H, Hwang H Y and Muller D A 2010 *Proc. Natl. Acad. Sci. USA* **107** 11682